Journal of New Technology and Materials (JNTM)
J. New Technol. Mater.
Vol. 08, N°02 (2018)77-82

OEB Univ. Publish. Co.

Effect of aluminum carbide additives on carbothermic reduction process from alumina to aluminum

Amina Chahtou[a], Rabie Benioub[a,b], Abderahmane Boucetta[a], Lihaowen Zeng[a], Hidekazu Kobatake[a,b] and Kenji Itaka[a,b,*]

[a] *Graduate School of Science and Technology, Hirosaki University, Hirosaki-shi, Aomori-kun, 036-8560, Japan*

[b] *North Japan Research Institute for Sustainable Energy, Hirosaki University, 2-1-3 Matsubara, Aomori, 030-0813, Japan*

*Corresponding author,itaka@hirosaki-u.ac.jp

Received date: Apr. 12, 2018; revised date: Nov. 28, 2018; accepted date: Dec. 15, 2018

Abstract

In terms of electricity consumption, the carbothermic reduction process of alumina (Al_2O_3) represents one of the promising candidates to overcome the current industrial Hall-Héroult process for the production of aluminum (Al) from Al_2O_3. The yield of the carbothermic reduction process of Al_2O_3, however, is not high enough to be considered as a substitute for the present industrial process. The calculation of the gas phase diagram of Al-O-C system suggests the possibility of the enhancement of the Al product yield by the increase of the ratio of the partial pressure Al_2O/CO. An increase in the ratio of the partial pressure Al_2O/CO can be expected by the reaction of aluminum carbide (Al_4C_3) and Al_2O_3. We investigated the effect of adding Al_4C_3 on the enhancement of the final Al yield in the production process. In the case without Al_4C_3 additive, the Al yield was only 1.4 %, while, in the case of adding Al_4C_3 additive with Al_2O_3: Al_4C_3 = 1:0.05 in molar ratio, the Al yield increased drastically up to 21.3 %.

Keywords: Alumina; Carbothermic reduction;Gas phase diagram;Aluminum;Aluminum carbide

1. Introduction

Aluminum metal is indispensable with various structural materials in automotive and aviation industries [1]. Industrially, aluminum is produced via the Hall-Héroult method in which aluminum metal is extracted by electrolysis of pure alumina (Al_2O_3) dissolved in cryolite NaF-AlF_3 solution. This conventional industrial process, however, expresses two main downsides, such as the requirement of high energy consumption and high greenhouse gases emission (CO_2, CF_4, and C_2F_6) [2-4].

Figure 1 shows the flow charts for Hall-Héroult process and carbothermic reduction process. The carbothermic reduction of Al represents one of the potential substitute methods for metal aluminum production due to its low consumption of electricity and minimal emission of greenhouse gases in comparison with the Hall-Héroult process [5-7]. In the carbothermic process of Al_2O_3, however, the generation of a lot of intermediate products such as aluminum carbide Al_4C_3 and oxy-carbide Al_2OC and Al_4O_4C and volatile aluminum suboxide Al_2O causes quite a low yield of the reduction process from alumina to aluminium [8-10].

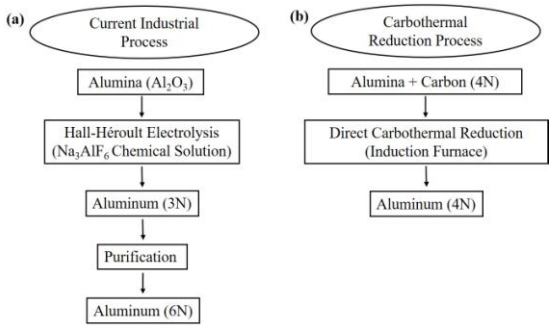

Figure 1 schematic comparison between current industrial process and carbothermic reduction process for the production of aluminum: (a) Hall-HéroultElectrolytic process and (b) our optimized carbothermic reduction process

Several research groups tried to improve the yield of the carbothermic reduction process via optimization of the experimental process itself. Investigation of the effect of different atmospheric gas (Ar, O_2, and CH_4) during the carbothermic reduction process on the final Al yield was performed [11]. Also, the generation temperature at which each phase of the reduction product appeared (Al_2O gas and solid forms, Al_4O_4C, Al_4C_3) was determined to emphasize the temperature effect on the yield of overall reduction reactions [12]. On the other hand, to investigate the impact of starting raw materials on the yield

enhancement, granules of alumina and carbon mixed with sugar powder as a binder were used [13].While other groups focused on the thermodynamic calculations of the phase diagram which led to studying of by-product behavior during the reduction process in a way to improve the yield [14-16]. However, the improvement of the Al yield by these trials was insufficient for a practical process.

The carbothermic reduction from alumina to aluminum is composed of a series of complicated processes under high-temperature through various intermediate products, such as Al_2O gaseous phase and solid forms Al_4O_4C, Al_4C_3. The complexity of these processes made the thermodynamic explanation and understanding of the different overall reactions behavior during the reduction process difficult. The main reason for the low Al yield in the product is due to the suboxide Al_2O gas loss because the Al_2O gas with sublimability is stable only at high temperature and is difficult to control in the furnace. However, the carbothermic reduction of Al_2O_3 is similar to the carbothermic reduction of silica (SiO_2) concerning the appearance of suboxide gas phase. In the case of silicon (Si), the thermodynamic gaseous phase diagram was utilized to understand the complicated reaction through the SiO gas phase and silicon carbide (SiC) solid phase [17, 18].

In this paper, we calculated the thermodynamic phase diagram with the partial pressure ratio of Al_2O and CO ($P(Al_2O)/P(CO)$). This diagram suggests the possibility of enhancement of Al yield by the increase of $P(Al_2O)/P(CO)$, which can be increased by the additive of Al_4C_3. We performed the optimization of Al_4C_3 additive under carbothermic reduction of Al_2O_3. At the optimal condition, the Al yield was improved 15 times as large as that without Al_4C_3.

2. Materials and Methods

2.1 Al-C-O Phase Stability Diagram

The carbothermic reaction from Al_2O_3 to Al are described as following equations:

$$Al_2O_3(s) + 2C(s) = Al_2O(g) + 2CO(g) \quad (1)$$

$$2Al_2O(g) + 5C(s) = Al_4C_3(s) + 2CO(g) \quad (2)$$

$$5Al_2O_3(s) + 2Al_4C_3(s) = 9Al_2O(g) + 6CO(g) \quad (3)$$

$$3Al_2O(g) + Al_4C_3(s) = 10Al(s) + 3CO(g) \quad (4)$$

Where (g) and (s) indicate the gas and solid phases, respectively. At first, Al_2O_3 reacts with carbon to generate Al_2O and CO gasses via reaction in Eq. (1). And then, Al_2O gas reacts with carbon to generate Al_4C_3 via reaction in Eq. (2). On the other hand, Al_2O_3 reacts with Al_4C_3 to generate Al_2O and CO gasses via reaction in Eq. (3). Finally, Al_4C_3 will react with Al_2O gas to generate Al metal via reaction in Eq. (4).

Only the reactions in Eqs. (1)(3) can generate the Al_2O gas. The ratio of partial pressure $P(Al_2O)/P(CO)$ corresponding to the reaction in Eqs. (1) and (3) are expressed in Table 1.

Table 1. comparison of the mol ratio between Al_2O and CO gasses generated from the reaction in Eqs. (1) and (3). In the case of reductant Al_4C_3, the ratio expresses a high ability to generate amount of Al_2O gas based on amount of CO gas

	P_a	P_b
Reductant to Al_2O_3	C	Al_4C_3
Reaction Eq. No	(1)	(3)
Mol. ratio (Al_2O/CO)	0.5	1.5

In Eqs. (2)and(4), the sum of coefficients for the gas phases (Al_2O and CO) on the reactant side equals to that on the product side. Under this restriction, two gas phases $P(Al_2O)$ and $P(CO)$ can be described by the ratio of partial pressures $P(Al_2O)$ and $P(CO)$ on the phase diagram, which is independent of the total pressure $P(Al_2O)$ + $P(CO)$.Figure 2 shows the gaseous phase diagram for the reactions in Eqs. (2) and (4), which were calculated with the standard Gibbs energy taken from MALT2 [19].

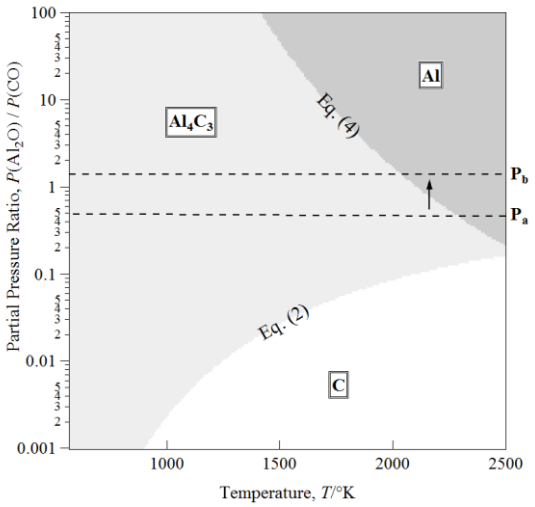

Figure 2. Thermodynamic calculation of phase stability diagram of Al_2O/CO gas phases for reactions in Eq. (1) and in Eq. (3), calculated with data from MALT2. $P_a$and P_b correspond to the partial pressure ratio $P(Al_2O)/P(CO)$ as shown in Table 1.

The horizontal dashed lines marked as P_a and P_b in Fig. 2 indicate partial pressure ratio as shown in Table 1. The phase diagram suggests that a largerratio of partial pressures $P(Al_2O)$ and $P(CO)$ can generate Al metal at a

lower temperature. Therefore, Al_4C_3 as an additive to raw materials will be expected to accelerate the Al generation.

2.2 Experimental Procedure

The Al_2O_3 powder (diameter 1μm, Kojundo Chemical Laboratory, Ltd) and glassy carbon powder (diameter 20 μm Tokai Carbon, Ltd) with a stoichiometric ratio of (Al_2O_3:C = 1:3 in molar ratio) were mixed as a base raw material. Then, Al_4C_3 additive powder was added in the range of 9 various molar ratios, from 0 to 0.1 molar ratio with a step of 0.01 of the starting raw material molar ratio.The mixtures were loaded to a high purity graphite crucible with an inner diameter of 40 mm and height of 70 mm covered with carbon felt and surrounded by quartz tube as an insulator and was installed in the center of the induction furnace as shown in Fig. 3.

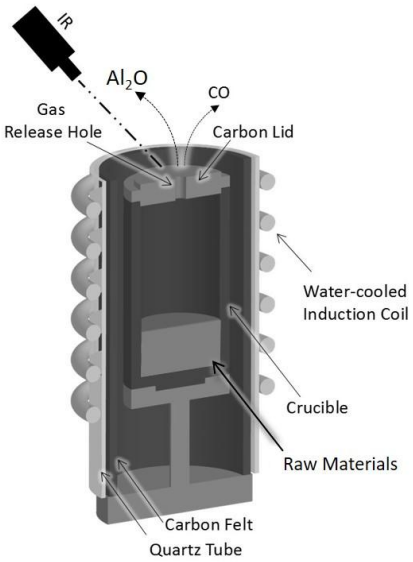

Figure 3. Schematic figure of the experimental apparatus. The carbon crucible was surroundedby thermal insulator (carbon felt) and quartz tube as electrical insulation

The Induction heating furnace is equipped with a highly sensitive color type infrared thermometer (IR-CAQ, CHINO Corporation, Japan) for continuous monitoring of the crucible temperature during the reduction process.

The atmosphere of the furnace was filled with Argon gas with a pressure of 0.09 MPa. All the samples were treated with the same temperature profile as shown in Fig. 4. The furnace was connected to the vacuum chamber with a quadrupole mass spectrometer through the small pin hole to convert the proper pressure. The base gas Ar was used to be a reference to estimate the partial pressure of CO gas.

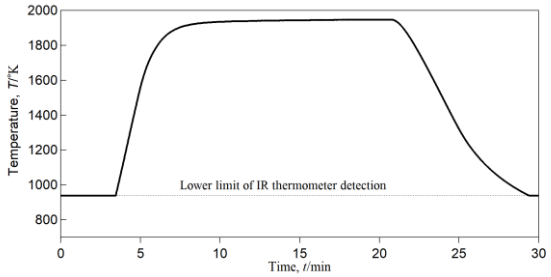

Figure 4. Typical temperature profile measured by the infrared thermometer during the reduction process. The lower limit of the infrared thermometer detection cannot measure the temperature below 925K.

2.3 Product Analysis Method

The phase of the product was analyzed using an *x*-ray diffraction system (SmartLab, Rigaku Corporation) with Cu-*Kα*(λ=1.5405Å) radiation source in the range of 20°≤2θ≤140° with a scan rate of 10°/minute using a 1D silicon strip detector (D/teX Ultra 250). To achieve precise quantification of the material in the product, Si powder was added as a reference to calculate the ratio of Al in products based on the internal standard method using the following equation[17]:

$$I_{(hkl)\alpha} / I_{(hkl)\beta} = q\,(X_\alpha / X_\beta) \quad (5)$$

where $I_{(hkl)\alpha}$ and $I_{(hkl)\beta}$ are the peak intensities of the sample and the Si standard, respectively. X_α and X_β are the weight fractions of the sample and the Si standard, respectively. The calibrationconstant $q$is estimated from the ratio of the *x*-ray peak intensities of $I_{(hkl)\alpha} / I_{(hkl)\beta}$as a function of ($X_\alpha / X_\beta$.), was 1.0682 for Al (200) based on Si (311). This calibration was used for quantification of Al_4O_4C, Al_4C_3, Al, $Al_2O_3$and C in the product.

3. Results and Discussions

3.1 Chamber Gas Analysis

Figure 5 shows the temporal change of the relative mass peaks (m/Z = 28) in the case of 0.05 molar ratio additive of Al_4C_3. The peak with m/Z = 28 represents residual N_2 gas and CO gas evolution during heating which mainly occurred due to the carbothermic reduction of alumina. This increase of CO gas was mainly generated from carbothermic reduction because residual N_2 gas is regarded as constant background.

The gas losses of CO and Al_2O were estimated in Eqs. (6) and (7) [18]:

$$M(CO)_{mol} = P_{furnace} * k * V_{furnace} / R * T_{furnace} \quad (6)$$

$$M(Al_2O) = (W_{loss} - M(CO)_{mol} * 28) / 70 \quad (7)$$

where R is gas constant, $P_{furnace}$, $V_{furnace}$, and $T_{furnace}$ are the pressure (Pa), volume (m^3) and temperature (K) of the total gas in the furnace. k is the ratio of the mass peak intensity between CO and Ar in quadrupole mass spectroscopy at the end of the reaction as shown in Fig. 5. The increase of the peak intensity of $m/Z = 28$ was used to estimate the factor k, which will be used for the estimation of Al_2O gas release during the reduction.

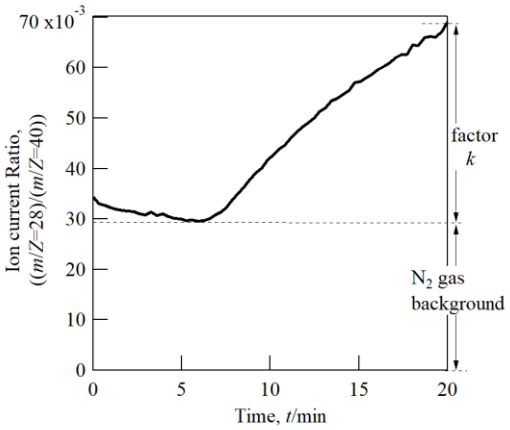

Figure 5. Real-time evolution of the released CO gas during the reduction process analyzed by quadrupole mass spectrometry. The background gas of N_2 is represented below the dashed line. The factor k was used for the calculation of Al_2O (mol) gas loss.

3.2. Product Analysis

3.2.1 Quantification of Products

Figure 6 shows the *x*-ray powder diffraction patterns for the milled products. An apparent effect of Al_4C_3 adding can be seen when comparing the different patterns related to progressive adding of Al_4C_3 molar ratio. A significant increase of the number and intensity of peaks corresponding to aluminum (Al) related to the progressive increase in mol% of Al_4C_3. The intermediate phases such as aluminum oxy-carbide (Al_4O_4C) appeared because of the incomplete reduction of Al_2O_3 to Al. The peaks related to Al_2O_3 and C represent the residual raw material due to incomplete reduction caused by gasses partial pressure inside the crucible or in case of only remains Al_2O_3 due to the exhaustion of carbon raw material. The carbon peaks can be explained by excess carbon powder or the graphite crucible. The excess of Al_4C_3 additives caused the decrease of Al content in the product as shown in Table 2. The peak intensities of the *x*-ray diffraction patterns were used for the quantification of the product using Eq. (5).

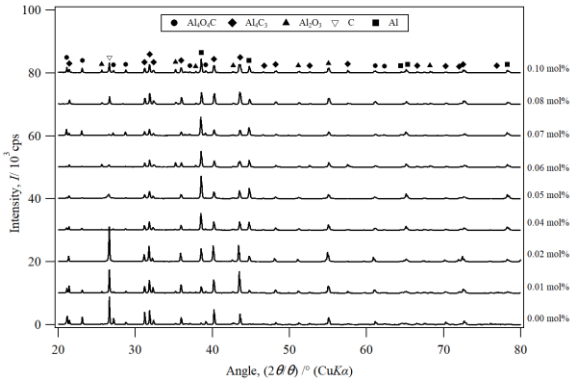

Figure 6. *x*-ray diffraction patterns of obtained products in the case of various additives (0 ~0.1 mol%)

3.2.2 Mass Balance

Table 2 shows the mass balance of the experimental results for the carbothermic reduction with the several different Al_4C_3 additives. Each column in Table 2 includes the amount of input raw materials, the product outputs, and weight loss gas. The Al product yield is defined as a molar ratio of Al element in the product and Al element in the input from Al_2O_3 raw material and Al_4C_3 additive.

Figure 7 shows Al yield as a function of the amount of Al_4C_3 additive. The total Al yield consists of Al element from two sources, Al_2O_3 raw material, and Al_4C_3 additives. The highest yield of Al with 21.3% was observed in the case with Al_4C_3 additive with Al_2O_3:Al_4C_3 = 1:0.05 in molar ratio, while the lowest yield of 1.4% was observed in the case without Al_4C_3 additive. In the case of more than 0.05 mol Al_4C_3additive, the total weight of solid product increased and the amount of intermediate product, Al_4O_4C and Al_4C_3, increased. This result indicates that the excess of Al_4C_3 additive caused the generation of the intermediate product, Al_4O_4C, andAl_4C_3.

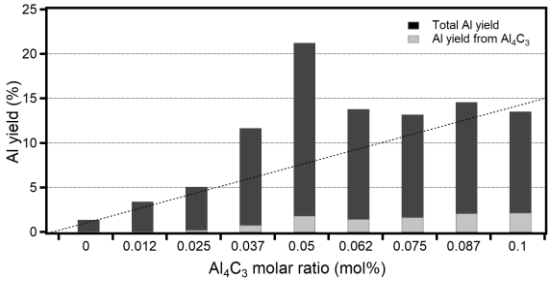

Figure 7. Total Al yield obtained from all samples. The percentage of Al yield from Al_4C_3 was estimated. The highest Al yield was obtained in sample 5 where 0.05 mol% of $Al_4C_3$was used.

Table 2. Mass balance for input raw materials and output product solid and gas phases shows a significant increase in the yield of Al corresponding to adding 0.05 molar ratio of Al_4C_3 as compared with other ratios. This comparison revealed the positive effect of Al_4C_3 additive for the production of Al.

		1		2		3		4		5	
		(g)	(Al mol)	(g)	(Al mol)	(g)	(Al mol)	(g)	(Al mol)	(g)	(Al mol)
Al_2O_3		14.800	0.290	14.800	0.290	14.800	0.290	14.800	0.290	14.800	0.290
C		5.210		5.210		5.210		5.210		5.210	
Al_4C_3		0.000	0.000	0.250	0.007	0.500	0.014	0.750	0.021	1.000	0.028
Total Input		20.010	0.290	20.250	0.297	20.510	0.304	20.760	0.311	21.010	0.318
Total Product		4.530	0.056	4.047	0.030	2.831	0.053	6.790	0.090	6.884	0.170
	Al	0.108	0.004	0.275	0.010	0.419	0.016	0.980	0.036	1.825	0.068
	Al_4C_3	0.155	0.004	0.241	0.007	0.181	0.005	0.180	0.005	0.169	0.005
	Al_4O_4C	0.006	0.0001	0.429	0.0093	1.172	0.0255	2.244	0.0488	4.480	0.0974
	Al_2O_3	2.442	0.048	0.180	0.004	0.351	0.007	0.000	0.000	0.000	0.000
	C	1.819		2.922		0.708		3.386		0.410	
Lost Gas		15.480		16.203		17.679		13.970		14.126	
	Al_2O	8.172	0.233	9.343	0.267	8.803	0.252	7.726	0.221	5.194	0.148
	CO	7.308		6.860		8.876		6.244		8.932	
Total Output		20.010	0.290	20.250	0.297	20.510	0.304	20.760	0.311	21.010	0.318
Al Yield (%)			1.378		3.428		5.103		11.670		21.257

		6		7		8		9	
		(g)	(Al mol)	(g)	(Al mol)	(g)	(Al mol)	(g)	(Al mol)
Al_2O_3		14.800	0.290	14.800	0.290	14.800	0.290	14.800	0.290
C		5.210		5.210		5.210		5.210	
Al_4C_3		1.250	0.035	1.500	0.042	1.750	0.049	2.000	0.056
Total Input		21.260	0.325	21.510	0.332	21.760	0.339	22.010	0.346
Total Product		11.253	0.197	8.381	0.207	8.638	0.077	11.220	0.200
	Al	1.214	0.045	1.184	0.044	1.336	0.049	1.265	0.047
	Al_4C_3	0.484	0.013	4.618	0.128	0.272	0.008	1.592	0.044
	Al_4O_4C	5.125	0.1114	0.467	0.0102	0.219	0.0048	2.089	0.0454
	Al_2O_3	1.375	0.027	1.274	0.025	0.769	0.015	3.232	0.063
	C	3.055		0.838		6.042		3.042	
Lost Gas		10.007		13.129		13.122		10.790	
	Al_2O	4.491	0.128	4.365	0.125	9.174	0.262	5.106	0.146
	CO	5.516		8.764		3.948		5.684	
Total Output		21.260	0.325	21.510	0.332	21.760	0.339	22.010	0.346
Al Yield (%)			13.838		13.214		14.605		13.551

If it is assumed that the whole Al_4C_3 additive was changed to Al metal perfectly, the dashed line indicates the expected value of the Al yield. The experimental results in the range from 0.037 to 0.087 mol Al_4C_3 additive, however, showed higher Al yield than the dashed line. Therefore, Al_4C_3 additive should have the effect to support the carbothermic reduction process from Al_2O_3 to Al. The Al yield from Al_4C_3 estimated from mass balance is at most 2.5%.

This assumption was which confirm that Al total yield is generated through Al_2O_3 reduction. The Al yield from Al_2O_3 was much larger than that from Al_4C_3 additive. If the reaction of Eq. (3) causes the increase of the $P(Al_2O)/P(CO)$, the enhancement of the Al yield by Al_4C_3 additive can be explained by the gaseous phase diagram, yield by Al_4C_3 additive is due to the increase of the $P(Al_2O)/P(CO)$.

Fig. 2. Although it is difficult to observe $P(Al_2O)$ directly in the capped carbon crucible because extracted Al_2O gas becomes solid below ~1000°C, our result strongly suggests that the possible explanation for the drastic change of Al

4. Conclusion

We calculated the Al-O-C gaseous phase diagrams for the carbothermic reduction of Al. This phase diagram suggests that importance of the ratio of partial pressure $P(Al_2O)/P(CO)$ to improve the Al yield for the carbothermic reduction process of Al_2O_3. The adding of Al_4C_3 additive to raw material, Al_2O_3 and carbon, was proposed as a way to increase the ratio of partial pressure $P(Al_2O)/P(CO)$. The effect of Al_4C_3 additive on the carbothermic reduction of $Al_2O_3$was investigated experimentally. In the case without Al_4C_3 additive, the Al yield was only 1.4 %, while, in the case of adding Al_4C_3additive with Al_2O_3:Al_4C_3 = 1:0.05 in molar ratio, the Al yield increased drastically by 15 times up to 21.3 %.

Acknowledgments

This research was supported by JST-JICA, SATREPS. A. Chahtou, R. Benioub and A. Boucetta gratefully acknowledge the scholarship from Ministry of Education, Culture, Sport, Science, and Technology (MEXT) of Japan.

References

[1] E. Balomenos, D. Panias, and L. Paspaliaris: Proc. Rev. Min. Proc. Extra Metall.32 (2011) 69-89.

[2] M. A. Rhamdhani, M. A. Dewan, G. A. Brooks, B. J. Monaghan, and L. Prentice: Proc. Rev. Min. Proc. Extra Metall. 122 (2013) 87-104.

[3] J. P. Murray: J. Sol. Energy Eng. 123 (2001) 125-132.

[4] T. E. Norgate, S. Jahanshahi, W.J. Rankin: J. Clean. Prod. 15 (2007) 838-848.

[5] E. Balomenos, D. Panias, L. Paspaliaris, B. Friedrich, B. Jaroni, A. Steinfeld, E. Guglielmini, M. Halmann, M. Epstein, I. Vishnevsky: Proc. EMC (2011) 729-743.

[6] E. Balomenos, I. Gianopoulou, D. Panias, I. Paspaliaris: J. Metalurgija15 (2009) 203-217.

[7] M. J. Bruno: Proc. Light Metals TMS. (2003) 395-400.

[8] R. J. Fruehan, Y. Li, and G. Carkin: J. Metall. Mater. Transac. B, 35 (2004) 617-623.

[9] P. Lefort, D. Tetard and P. Tristant: J. Euro. Ceram. Soc. 12 (1993) 123-129.

[10]J. H. Cox and L.M. Pidgeon: Can. J. Chem. 41 (1963) 671-683.

[11] M. Halmann, A. Ferai, A. Steinfeld: Energy 32 (2007) 2420–2427.

[12]M. Halmann, A. Steinfeld, M. Epstein, E. Guglielmini, I. Vishnevetsky: Conf. ECOS. (2012).

[13] M. Krusai, M.E. Galvez, M. Halmann, and A. Steinfeld: J. Metall. Mater. Transac. B, 42 (2011) 254-260.

[14] Y. Qing-chun, Y. Hai-bin, Z. Fu-long, Zhang Han, W. Chen, L. Da-chun, Y. Bin: J. Cent. South Univ. 19 (2012) 1813-1816.

[15] J. M. Lihrmann: J. Europ. Ceram. Soc. 28 (2008) 633-642.

[16] J. M. Lihrmann: J. Europ. Ceram. Soc. 28 (2008) 649-656.

[17] A. Boucetta, R. Benioub, A. Chahtou, S. M. Heddadj, T. Ogasawara, Y. Furuya, S. Hamzaoui, K. Itaka: Mater. Trans. 57 (2016) 1936-1944.

[18] R. Benioub, A. Boucetta, A. Chahtou, S. M. Heddadj, M. Adnane, Y. Furuya and K. Itaka: Mater. Trans. 57 (2016) 1930-1935.

[19] H. Yokokawa, S. Yamauchi, T. Matsumoto: Calphad26 (2002) 155-166.